PROCEEDINGS OF SCIENCE

Analysis of local and nonlocal amplitudes in the $B^0 \to K^{*0}\mu^+\mu^-$

Zahra Ghorbanimoghaddam[a,*] **On behalf of LHCb collaboration**

[a] *University of Bristol,*
HH Wills Physics Laboratory, Tyndall Avenue, Bristol BS8 1TL, UK

E-mail: zahra.ghorbani.moghaddam@cern.ch

The $B^0 \to K^{*0}\mu^+\mu^-$ decay occurs via the rare flavor-changing neutral current (FCNC) transition $b \to sl^+l^-$, making it a sensitive probe for New Physics (NP) since FCNC is forbidden at tree level in the Standard Model (SM). Virtual NP contributions can significantly influence this decay, and previous LHCb measurements have shown notable discrepancies with SM predictions at a 3σ level. Interpreting these anomalies is challenging due to uncertainties in nonlocal SM contributions, such as charm-loops, which can mimic NP effects. This contribution covers results from a data-driven approach aimed at determining the size of charm-loops and other nonlocal contributions to the $B^0 \to K^{*0}\mu^+\mu^-$ amplitude. This is the first measurement to parametrize the full dimuon invariant mass spectrum, using an integrated luminosity of 8.4fb^{-1} collected by the LHCb experiment.

The 43rd International Symposium on Physics in Collision - PIC 2024 ,
22-25 October 2024 ,
NCSR, "Demokritos", Athens, Greece

*Speaker

© Copyright owned by the author(s) under the terms of the Creative Commons Attribution-NonCommercial-NoDerivatives 4.0 International License (CC BY-NC-ND 4.0) All rights for text and data mining, AI training, and similar technologies for commercial purposes, are reserved. ISSN 1824-8039 . Published by SISSA Medialab.

PoS(PIC2024)021

1. Introduction

The analysis of $b \to sl^+l^-$ flavor-changing neutral current (FCNC) decays is a powerful tool for testing the Standard Model (SM). These decay processes are highly sensitive to potential new physics (NP) due to their extremely suppressed nature within the SM. Consequently, NP contributions at the tree level can compete with the suppressed SM processes at the loop level, and their combined effects can be indirectly measured through shifts in various observables relative to SM values. Since FCNC processes are sensitive to both local and nonlocal physics, performing precision measurements is crucial to distinguish these effects from non-SM physics. For instance, previous angular analyses of these decays have shown an overall discrepancy with respect to SM prediction at the level of three standard deviations (3σ) [1]. This analysis introduces a detailed model to simultaneously describe the rare $B^0 \to K^{*0}\mu^+\mu^-$ decay and the contributions of nonlocal effects across the full q^2 spectrum. Studying these nonlocal contributions is essential for understanding the interference effects between resonance contributions and the suppressed FCNC process. Such studies will ultimately help us discriminate between tensions arising from new physics (NP) effects and unaccounted-for SM physics.

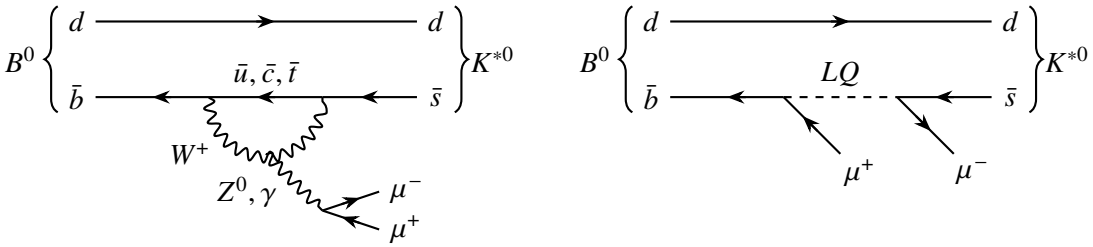

2. Theoretical Framework

The weak effective theory is an essential framework in particle physics for describing weak interactions at low energies. By integrating out heavy degrees of freedom, this approach simplifies the complex interactions of the Standard Model,

$$\mathcal{H}_{WET} = \frac{4G_F}{\sqrt{2}} V_{tb} V_{ts}^* \sum_i (C_i^{(\prime)}(\mu) O_i^{(\prime)}(\mu)) \tag{1}$$

This approach focuses on effective interactions between remaining particles, making it useful for studying FCNCs. The effective Hamiltonian uses an operator product expansion (OPE) to describe interactions through effective operators and corresponding Wilson coefficients in which high-energy physics effects are encapsulated. Quark transitions are described by the Cabibbo-Kobayashi-Maskawa (CKM) matrix elements and the Fermi constant (G_F) constant, while the Standard Model includes local interaction couplings such as the electromagnetic coupling (C_7), the vector coupling (C_9) and the axial-vector coupling (C_{10}), nonlocal contributions come from four-quark operators $O_{1,2}$, which produce a dimuon pair via the electromagnetic current, dominated by the charm-loop operator ($b \to sc\bar{c} \to \gamma^* \to \mu^+\mu^-$). These operators mix with $O_{7,9}$ through renormalization, resulting in observables sensitive to effective operators, $O_{7,9}^{\text{eff}}$, and their corresponding effective Wilson coefficients $O_{7,9}^{\text{eff}}$. Results from various analyses of the same transition can be

PoS(PIC2024)021

interpreted using these effective couplings through global fits of model-independent measurements. For instance, measurements of $b \to s\mu^+\mu^-$ processes show a shift of approximately 3σ for C_9 from the Standard Model value, Fig.1[1]. The 5-D differential decay rate of $B^0 \to K^{*0}(\to K^+\pi^-)\mu^+\mu^-$

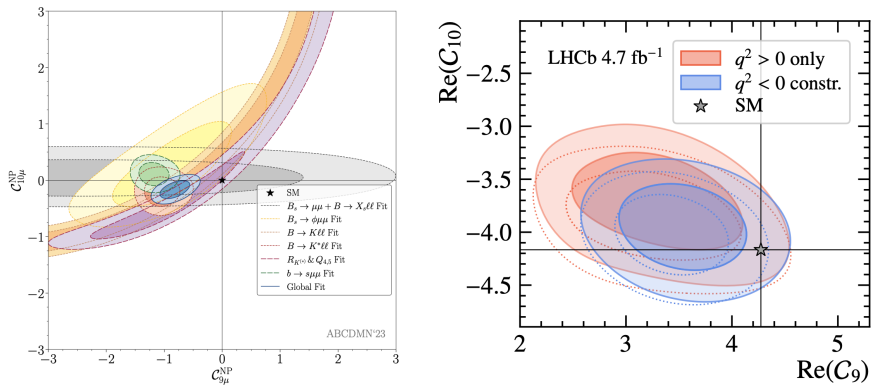

Figure 1: Results of C_{10} and C_9 from (left) the global fit performed in Ref.[1], and the z-expansion analysis [2] w/wo theory input constrain at negative q^2.

can be expressed as follows:

$$\frac{d^5\bar{\Gamma}(B^0 \to K^+\pi^-\mu^+\mu^-)}{dq^2 d\vec{\Omega} dm^2_{K\pi}} = \frac{9}{32\pi}\sum_i \bar{J}_i(q^2)\mathcal{F}_i(\cos\theta_l, \cos\theta_K, \phi)\mathcal{G}_i(m^2_{K\pi}) \tag{2}$$

Where J_i are the q^2-dependent angular coefficients and $\mathcal{F}_i$ are the spherical harmonic angular functions depending on three helicity angles that define the decay geometry (see Fig. 2). $J_i(q^2)$ contains all the transversity amplitudes, previously measured in binned analyses [5], including the angular observables. For example, the well-known P'_5 [1] can be constructed from a combination of these angular observables in a way that minimizes the uncertainties of the hadronic contributions. Additionally, $\mathcal{G}_i$ is a function in the K^{*0} system that includes the bilinear product of the line shapes of S- and P- wave amplitudes. The P-wave line shape is modeled using a relativistic Breit–Wigner

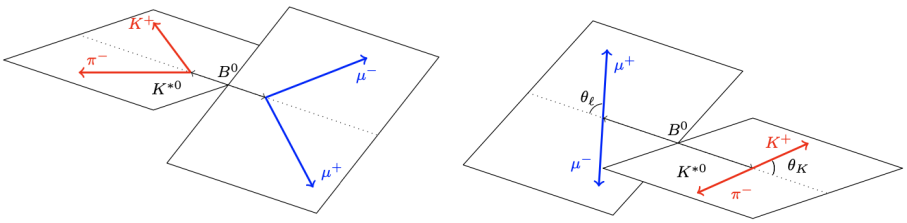

Figure 2: Geometry of the decay as per LHCb convention.

function, while for the S-wave line shape the LASS parametrization is followed [2] . The K^{*0} system's contribution is integrated over $0.796 < m_{K\pi}[\text{ GeV}/c^2] < 0.996$ due to the suppressed q^2 dependence of $\mathcal{G}_i$. The $J_i(q^2)$ angular functions include form factors (FF), with local contributions

[1] $P'_5 = \frac{S_5}{\sqrt{F_L(1-F_L)}}$ where F_L is the longitudinal polarization fraction of K^{*0}, and S_5 is a CP-symmetric angular observable

PoS(PIC2024)021

described by Light-Cone Sum Rules (LCSR) [3] and Lattice QCD (LQCD) [4]. Nonlocal FF are absorbed into the q^2 and polarization(λ)-dependent effective Wilson coefficients $C^{\text{eff},\lambda}(q^2)$. A previous LHCb analysis [2] of data from Run 1 and 2016 (4.7 fb^{-1}) modeled nonlocal contributions through a polynomial expansion in a limited q^2 region. Results on vector and axial-vector couplings, with and without constraints at negative q^2, show minimal impact of nonlocal contributions on the previously observed shift in the vector coupling (see Fig. 1).

3. Analysis Strategy

This analysis fits LHCb data with a model that, for the first time, combines local and nonlocal amplitudes across a broad q^2 spectrum ($0.1 \leq q^2[\text{ GeV}^2/c^4] \leq 18.0$). The model includes all known resonances couple to the dimuon final state through a dispersion relation model, determining the nonlocal contributions and Wilson coefficients simultaneously. The transversity amplitudes that make up the angular observables $J_i(q^2)$ are parameterized for various polarizations of the K^{*0}, incorporating both local and nonlocal effects.[2] For instance, the explicit form of one $J_i(q^2)$ reads:

$$J_5(q^2) \propto \sqrt{2}\beta_\ell \left(\text{Re}\left(A_0^L A_\perp^{L*} - A_0^R A_\perp^{R*}\right)\right)$$

where the amplitudes can be written in a general way:

$$A_\lambda^{L,R}(q^2) = N_\lambda((C_9^{\text{eff},\lambda} \pm C_9') \mp (C_{10} \pm C_{10}'))F_\lambda^A(q^2) + M_\lambda C_7^{\text{eff},\lambda} F_\lambda^T(q^2) \tag{3}$$

which includes the normalization factors, N_λ and M_λ, local hadronic form factors $F_\lambda^A(q^2)$ and $F_\lambda^T(q^2)$. While the $C_7^{\text{eff},\lambda}$ and $C_9^{\text{eff},\lambda}$ represent the left-handed effective couplings, the right-handed couplings C_9' and C_{10}', despite being highly suppressed in SM, are included in order to increase NP potential sources. The nonlocal contributions are modeled by a subtracted dispersion relation, $Y^{q\bar{q},\lambda}(q^2)$ [6]:

$$C_9^{\text{eff},\lambda} = C_9 + Y_{light}^{1P}(q^2) + \sum_{n=1P,2P} Y_{c\bar{c}}^{n,\lambda}(q^2) + Y_{\tau\bar{\tau}}(q^2)$$
$$C_7^{\text{eff},\lambda} = C_7 + \xi^\lambda e^{i\omega^\lambda},$$

where the nonlocal vector contributions include one-particle and two-particle states[3]. One-particle states include light resonances, $\rho(770)$, $\omega(782)$, and $c\bar{c}$ resonances $\phi(1020)$, J/ψ, $\psi(2S)$, $\psi(3770)$, $\psi(4040)$, $\psi(4160)$. Two-particle states include open-charm $D^{(*)}\bar{D}^{(*)}$[4] and $\tau^+\tau^-$ loop. The effective coupling C_9^τ can be directly measured through re-scattering of $B^0 \to K^{*0}\tau^+\tau^-(\to \mu^+\mu^-)$.

The signal candidates are identified through a combination of hardware and software triggers, as well as offline selections, and are reconstructed and modeled in four dimensions ($\cos(\theta_l)$, $\cos(\theta_k)$, ϕ, q^2) (4D)(see Fig.3). An unbinned maximum likelihood fit is performed in 4D simultaneously across three q^2 regions (see Fig.4)[5]. Significant background contributions, primarily from combinatorials (random combinations of kaons, pions, and muons from random parent particles) are reduced by applying a Boosted Decision Tree (BDT) [6].

[2] These can be written as six amplitudes: $A_0^{L,R}$, $A_\perp^{L,R}$, $A_\parallel^{L,R}$ [6].

[3] C_7^{eff} is subject solely to vertex corrections, resulting in a polarization-dependent shift. [6]

[4] Our current model does not explicitly account for re-scattering amplitudes such as $B \to D_s D^* \to K^*\mu^+\mu^-$ [6]. Ref.[8] and Ref.[7] demonstrate latest developments

[5] All fit projections have been performed simultaneously in three q^2 regions: low [0.10, 3.24], mid [3.24, 11.56], and high [11.56, 18.00]

PoS(PIC2024)021

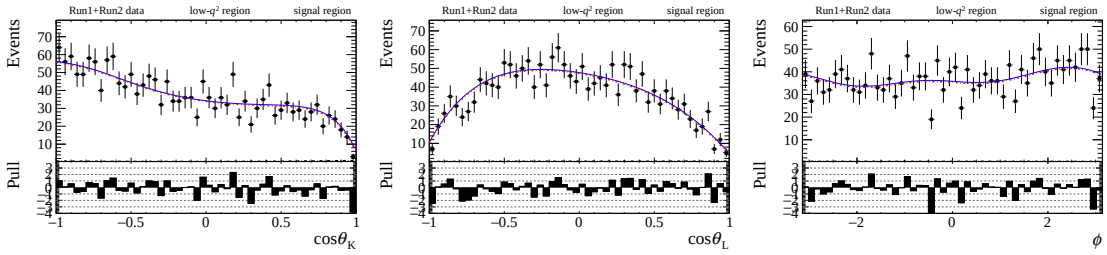

Figure 3: Fit projections for three helicity angles shown for rare-mode dominated region (low q^2)

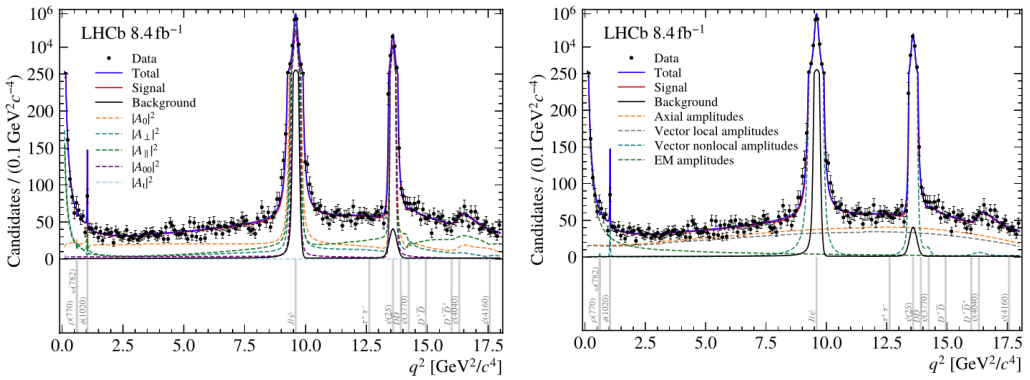

Figure 4: The q^2 distribution in the data, overlaid with the PDF projection from the baseline fit. The total PDF is decomposed into signal and background components, with the signal contributions from the different transversity amplitudes (left) and various Lorentz structures (right).

4. Results

In this work, a comprehensive amplitude analysis of the decay $B^0 \to K^{*0}\mu^+\mu^-$ has been performed over the q^2 range $[0.10, 18.00]$ GeV$^2/c^4$ for the first time using LHCb data from Run 1 and 2 (8.4 fb^{-1}). The data, overlaid with the baseline fit, demonstrate the various contributions of the signal, non-local effects, interferences, transversity amplitudes, and combinatorial backgrounds (see Fig. 4). The impact of non-local contributions on Wilson coefficients shows a non-negligible shift from the Standard Model (SM) expectation value for $\Delta C_9 \approx -0.7$ (see Fig. 5), while the effect on other WCs is not significant. Although this result [6] is in good agreement with the z-expansion analysis in Ref. [2] (see Fig. 5), it shows less compatibility with results using theory input at negative q^2. Despite the larger-than-expected non-local contributions in previous measurements, the full shift in C_9 of 2.1σ and a global tension of 1.5σ relative to the SM remain unexplained. Moreover, no significant q^2 dependence has been observed in C_9. The indirect measurement of the $B^0 \to K^{*0}\tau^+\tau^-$ process through dimuon re-scattering marks the first direct measurement of the $bs\tau^+\tau^-$ effective coupling, C_9^τ, which is $(1.0 \pm 2.6 \pm 1.0) \times 10^2$. The sensitivity from this re-scattering measurement is comparable to that of direct searches for the $B^0 \to K^{*0}\tau^+\tau^-$ process [10]. The dominant systematics arises from normalization relative to the $B^0 \to J/\psi K^{*0}$ decay, due to the uncertainty in the measured branching fraction for this decay mode [9].

PoS(PIC2024)021

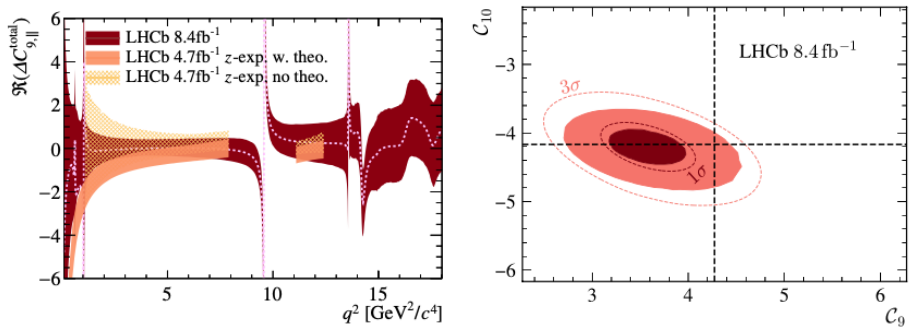

Figure 5: Impact from the nonlocal contributions (left) from the parallel polarization of the K^{*0} on $Re(C_9)$, the results are overlaid with z-expansion (w/wo theory input). Dispersion model results (right) shows 1σ and 3σ regions. Shaded contours account for only statistical uncertainties while the dashed line includes systematic uncertainties as well.

References

[1] M. Algueró et al., *To (b)e or not to (b)e: no electrons at LHCb*, Eur.Phys.J.C 83 (2023) 7, 648

[2] LHCb collaboration, R. Aaij et al., *Determination of short- and long-distance contributions in decays, Phys. Rev. D109 (2024) 052009, arXiv:2312.09102*

[3] N. Gubernari, A. Kokulu, and D. van Dyk, *$B \to P$ and $B \to V$ form factors from B-Meson Light-Cone Sum Rules beyond leading twist*, JHEP 01 (2019) 150, arXiv:1811.00983

[4] R. R. Horgan, Z. Liu, S. Meinel, and M. Wingate, *Rare B decays using lattice QCD form factors*, PoS LATTICE2014 (2015) 372, arXiv:1501.00367

[5] LHCb Collaboration, R. Aaij et al., *Measurement of CP-Averaged Observables $B^0 \to K^{*0}\mu^+\mu^-$ Decay*, Phys. Rev. Lett. 125, 011802

[6] LHCb Collaboration, R. Aaij et al., *Comprehensive analysis of local and nonlocal amplitudes in the $B^0 \to K^{*0}\mu^+\mu^-$ decay*, JHEP 09 (2024) 026

[7] Gino Isidori, Zachary Polonsky, Arianna Tinari, *An explicit estimate of charm rescattering in $B^0 \to K^0 l\bar{l}$*, arXive.2405.17551v1

[8] C. Cornella et al., *Hunting for $B^+ \to K^+\tau^+\tau^-$ imprints on the $B^+ \to K^+\mu^+\mu^-$ dimuon spectrum*, Eur.Phys.J.C80(2020) 1095

[9] Belle Collaboration, K. Chilikin et al., *Observation of a new charged charmoniumlike state in $\bar{B}^0 \to J\psi K^-\pi^+$ decays*, Phys. Rev. D90 (2014) 112009

[10] Belle Collaboration, K. Chilikin et al., *Search for the $B^0 \to K^{*0}\tau^+\tau^-$ decay at the Belle experiment*, Phys. Rev D108 (2023) L011102

PoS(PIC2024)021